

A field study to understand the currents and loads of a near shore finfish farm

David W. Fredriksson

Department of Naval Architecture and Ocean Engineering
United States Naval Academy, Annapolis, MD 21402

Judson C. DeCew

Center for Ocean Engineering
University of New Hampshire, Durham NH 03824

James D. Irish

Department of Applied Ocean Physics and Engineering
Woods Hole Oceanographic Institution, Woods Hole, MA 02543

Abstract- An extensive field study was conducted to investigate the current velocities and mooring system tensions in a 20-unit net pen fish farm located in Eastport Maine, USA, near the Bay of Fundy where extreme tides create strong currents loading fish farm components. To understand the flow characteristics at the site, currents meters were deployed at external and internal farm locations during three distinct operational conditions: (1) clean nets for smolts, (2) clean nets for standard grow out and (3) nets for standard grow out at the end of the stocking schedule, when the gear is fouled with biological material. Also, several load cells were deployed at the same time on important anchor leg and net pen attachment components to measure system loads. The current meter data sets provided evidence of velocity flow reduction through the farm by examining the current meter statistics and tidal harmonic constituents. Tidal analysis also showed substantial tidal harmonics or shallow water tides. The load cells measured maximum loads of 104 kN for anchor leg and 11 kN for net pen lines. The results are significant because few extensive fish farm engineering data sets exist, especially for different combinations of nets and levels of biological fouling. These results are being used in complementary studies to quantify flow reduction, to validate Morison equation type numerical models and as a baseline for specifying offshore fish farm gear.

I. INTRODUCTION

The design of near shore fish farms has evolved over the past decades from small wooden rafts, to articulated steel, “dock-like” platforms, and to flotillas of containment structures (net pens) made often from High Density Polyethylene (HDPE) flotation pipe with suspended nets. In these near-shore environments, the sites are typically sheltered from extreme waves but still subjected to tidal currents and storm forced events. In many areas, the development of mooring systems and net pen gear has been determined from trial and error resulting from failures and loss of equipment and product. Engineering research in this field has focused on the hydrodynamic characteristics and modeling of nets [1], [2], and [3], force calculation on cages and farms [4], [5], and [6], and

physical modeling of systems [7], [8] and [9]. Some researchers have also published field measurements of loads and motions. [10] investigated wave-induced loads on a multi-cage (near shore) farm. The development of the appropriate instrumentation for fish farm engineering measurement studies was done by [11]. While [8], [12], [13], and [14] reported motions and loads for one fish cage type.

As near shore sites become more difficult to operate due to multi-use issues, many are considering exposed or open ocean locations. The design of large fish farms for high energy environments is not trivial since a balance must exist between cost-effectiveness and robust components. “Over engineering” may not be an option in an industry where profit margins can be small. Engineering design techniques need to be developed systematically and validated. One validation approach is to utilize full scale measurements.

The objective of this study is to develop field measurement techniques and obtain detailed current velocity forcing and mooring tension data at a large fish farm in full operation. The information is being used to understand dominating physical parameters, for future work analyzing flow field characteristics and to validate Morison equation models for component specification. To understand the flow characteristics at the site, current meters were deployed outside the farm to identify the forcing on the net pens and mooring lines, and at interior locations to measure the changes in currents behind the net pens. Also, load cells were used to measure critical anchor-leg and pen attachment line tensions. The measurements were made during three operational conditions characteristic of the salmon grow out process where different types of nets are installed and levels of biological fouling existed. This paper is organized to include a description of the fish farm system, the instrumentation particulars and deployment scheme, data results and design implications.

II. SITE DESCRIPTION

A. Farm Location

The near shore fish farm is located in Broad Cove, Eastport

Funding was provided by the National Oceanic and Atmospheric Administration Saltonstall-Kennedy funding under Grant NAO3NMF4270183.

Report Documentation Page

Form Approved
OMB No. 0704-0188

Public reporting burden for the collection of information is estimated to average 1 hour per response, including the time for reviewing instructions, searching existing data sources, gathering and maintaining the data needed, and completing and reviewing the collection of information. Send comments regarding this burden estimate or any other aspect of this collection of information, including suggestions for reducing this burden, to Washington Headquarters Services, Directorate for Information Operations and Reports, 1215 Jefferson Davis Highway, Suite 1204, Arlington VA 22202-4302. Respondents should be aware that notwithstanding any other provision of law, no person shall be subject to a penalty for failing to comply with a collection of information if it does not display a currently valid OMB control number.

1. REPORT DATE 01 SEP 2006		2. REPORT TYPE N/A		3. DATES COVERED -	
4. TITLE AND SUBTITLE A field study to understand the currents and loads of a near shore finfish farm				5a. CONTRACT NUMBER	
				5b. GRANT NUMBER	
				5c. PROGRAM ELEMENT NUMBER	
6. AUTHOR(S)				5d. PROJECT NUMBER	
				5e. TASK NUMBER	
				5f. WORK UNIT NUMBER	
7. PERFORMING ORGANIZATION NAME(S) AND ADDRESS(ES) Department of Naval Architecture and Ocean Engineering United States Naval Academy, Annapolis, MD 21402				8. PERFORMING ORGANIZATION REPORT NUMBER	
9. SPONSORING/MONITORING AGENCY NAME(S) AND ADDRESS(ES)				10. SPONSOR/MONITOR'S ACRONYM(S)	
				11. SPONSOR/MONITOR'S REPORT NUMBER(S)	
12. DISTRIBUTION/AVAILABILITY STATEMENT Approved for public release, distribution unlimited					
13. SUPPLEMENTARY NOTES See also ADM002006. Proceedings of the MTS/IEEE OCEANS 2006 Boston Conference and Exhibition Held in Boston, Massachusetts on September 15-21, 2006. Federal Government Rights, The original document contains color images.					
14. ABSTRACT					
15. SUBJECT TERMS					
16. SECURITY CLASSIFICATION OF:			17. LIMITATION OF ABSTRACT UU	18. NUMBER OF PAGES 9	19a. NAME OF RESPONSIBLE PERSON
a. REPORT unclassified	b. ABSTRACT unclassified	c. THIS PAGE unclassified			

Maine, USA, near the Canadian boarder. The site is well protected from waves generated in the Gulf of Maine by Campobello and Grand Manan Islands. However, the extreme tidal elevations in the Bay of Fundy, due to the near resonance of the Gulf of Maine-Bay of Fundy system [15] cause ± 4 m spring tidal elevations at the site. Strong tidal currents [16], are the principle forcing on the farm components.

B. Mooring System

The farm (Fig. 1) consists of 20 net pens each with a radius of 15.9 m connected to a near-surface mooring grid with 26 anchor legs (Fig. 2). The mooring grid is located at a depth of ~ 5 m and is held up off the bottom with flotation elements on each anchor leg consisting of 1.8-meter diameter steel balls (Fig.3). The anchor legs are mostly chain and extend down to the bottom beneath the floats and the grid to the anchors (Fig. 3). The dimensions of the farm as contained by mooring grid surface floats are approximately 274 by 219 meters. The specific focus area of study was situated around the most South-west net pen shown on Figs. 1 and 2

C. Net Pen Structure

The structures that are used to contain the fish at the farm are typical gravity type net pens constructed from circular pipe made of HDPE with a circumference of 100 meters. Two sets of circular ringed pipes are used as the primary components of the pen. At the surface, the two concentric rings are connected together and serve as flotation (filled with air) from which containment and predator nets are hung (Fig. 4). The surface ring structure also incorporates additional pipe sections that form a “handrail” so it can be used as a work platform. Additional pipes (not shown on Fig. 4) are filled with either sand or concrete and used as weight rings attached to the bottom part of the nets to form the volumetric characteristics of the pen. Also, netting over the pens prevents loss of fish to birds. In the center of each pen is a feeding system

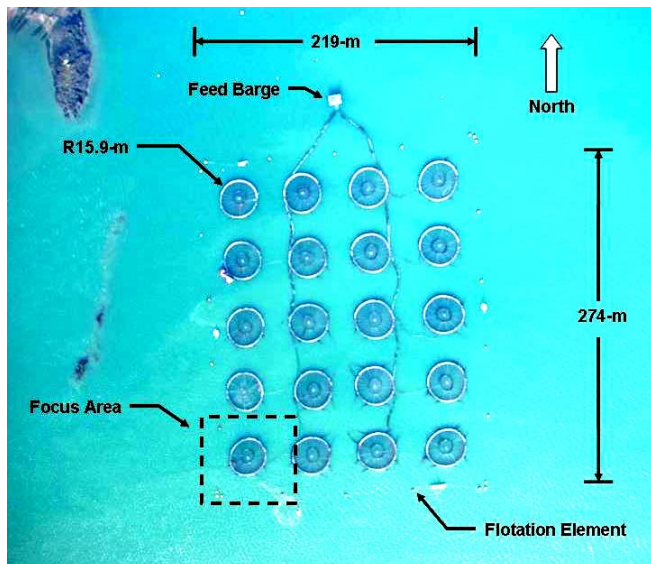


Figure 1: An aerial photograph of the 20 net pens deployed at the farm site in Broad Cove (photo courtesy of Card’s Aquaculture).

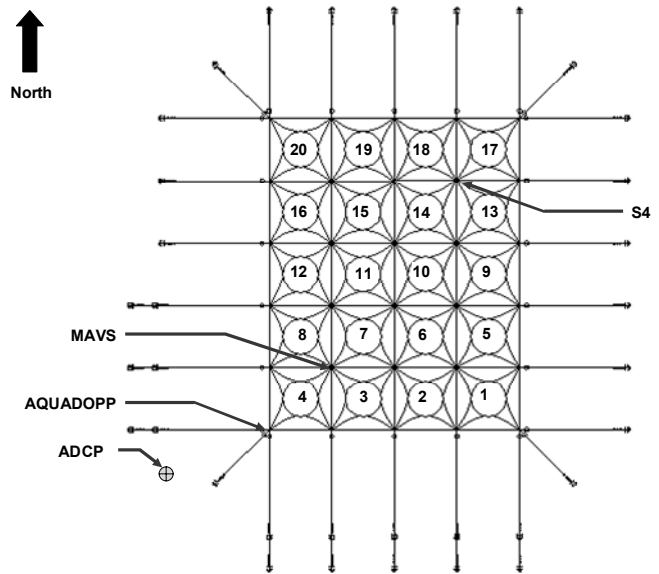


Figure 2: The net-pens are numbered from 1 to 20, the anchors, mooring grid and the deployment location for each of the current meters shown.

connected by floating hoses (Fig. 1), to a feed barge moored north of the farm which can be seen running to each net pen.

D. Operational Conditions

The measurement study was conducted under three different operational conditions, typical of many near shore farm facilities, (1) clean containment and predator nets for smolts, (2) clean containment and predator nets for standard grow-out and (3) containment and predator nets for standard grow-out at the end of the stocking schedule, (16-18 months) when the gear is typically fouled with biological material. The net twine diameter, spacing, and solidity characteristics for these three conditions are provided in Table 1. The solidity is defined at the ratio between the actual projected net material area to the outline area of a panel. For conditions #2 and #3 the net characteristics are the same, however, the solidity for condition #3 was difficult to quantify since the nets were fouled with biological material. For conditions #1 and #2, the total net solidity is also provided in Table 1.

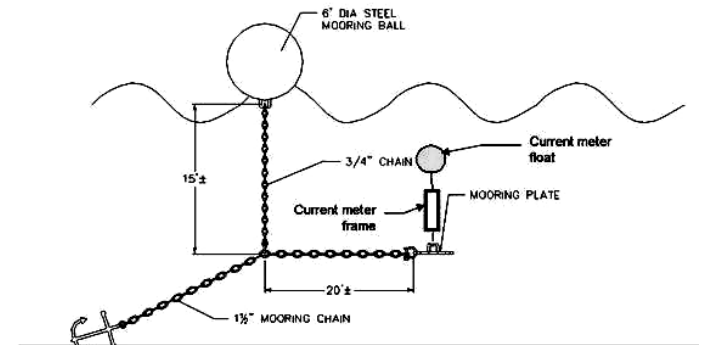


Figure 3: The mooring grid with anchor, mooring chain, and float configuration. The AQUADOPP, MAVS and S4 current meters were attached to the mooring grid and positioned in the water column about mid-depth of the net-pens.



Figure 4: A net pen deployed at the Broad Cove site. Note the fouling of the net pen attachment line with floating debris in the foreground.

Table 1: The net twine diameter and spacing characteristics used for each operational condition. Net solidity information is also included.

Condition	#1	#2	#3
Predator Net			
Twine Diameter (mm)	3.25	3.25	3.25
Knot-to-Knot Spacing (mm)	102	102	102
Solidity (%)	6.4	6.4	n.a. ¹
Fish (Containment) Net			
Twine Diameter (mm)	-	2.0	2.0
Knot-to-Knot Spacing (mm)	-	30.2	30.2
Solidity (%)	-	13.3	n.a. ¹
Smolt Net			
Twine Diameter (mm)	3	-	-
Knot-to-Knot Spacing (mm)	17.5	-	-
Solidity (%)	34.4	-	-
Total Net Solidity (%)	40.8	19.7	n.a.¹

¹During operational condition #3, the nets were fouled heavily with biological material.

III. INSTRUMENTS

A. Current Meters

Multiple current meters were deployed at the Broad Cove site with at least one positioned outside of the farm to measure current forcing uncontaminated by farm effects. Interviews with operational personnel indicated that the strongest tidal currents typically flow in the West-Northwest and East-Southeast directions. Historically, the net pen that “experienced” the most wear was pen #4 (Fig. 2) located in the Southwest corner.

An RD Instruments ADCP (Acoustic Doppler Current Profiler) was deployed ~75 m to the Southwest (seaward) side of net pen #4. It was moored on a subsurface float (Fig. 5) farthest from the cage (Figs. 2 and 6). The ADCP uses acoustic Doppler techniques to measure velocities, and makes profiles by range gating the returned signals into 40 bins each with a vertical size of 0.5 meters. Being moored to the bottom, the ADCP made measurements relative to the bottom, while the other current meters made measurements relative to the water surface. The ADCP was only deployed during condition #3 (fouled case) because the farm operational staff feared that a local dragger was targeting the deployment site.

At approximately 23 m to the SW of net pen #4, a Nortek AQUADOPP current meter was deployed, closer to the fish

farm than the ADCP, but still outside the farm (Figs. 2 and 6). The AQUADOPP was used for all three deployments at this location as a measure of the current forcing on the farm. This instrument measured the current velocity by Doppler techniques. The measurement volume was made approximately 1.3 meters away from the sensor to reduce the flow disturbance from the sensor housing and mooring. The AQUADOPP also recorded temperature, pressure (for depth), roll, pitch and heading, which were used to calculate velocities in earth coordinates. The orientation data also provided information on current meter motion to evaluate data quality.

A Nobska MAVS current meter was deployed approximately 23 m to the NW of pen #4 toward pen #7 (Figs. 2 and 6). The MAVS current meter was placed at this location for all three deployments in an effort to acquire data that would “shed light” on the differences between undisturbed flow on the outside of the system to the flow characteristics behind the southwest net pen. The MAVS current meter uses differential travel time measurements to estimate velocity. A disadvantage of the MAVS is that it is subject to biological fouling which can reduce the flow through the sensing volume. The MAVS also records temperature, tilt and orientation, and provided velocity in earth coordinates.

An Interocean S4 current meter, was deployed between pen #14 and #17 (Figs. 2 and 6) during condition #1 (when smolt nets were deployed). The instrument was placed on the opposite side of the farm to investigate far field current velocity differences. The S4 current meter uses the water flow velocity as a conductor through a magnetic field created by the instrument. The voltage change measured on opposite sides of the instrument in the magnetic field is proportional to the flow velocity. The S4 current meter measures the two horizontal velocity components and records them in earth coordinates.

The current meters (except the ADCP) were placed at a depth about ½ that of the cage (the actual depth change of the instrument was within 2 m during a tidal cycle). Each current meter was attached to the mooring grid near mooring plates



Figure 5: The ADCP in mooring frame with white flotation spheres during deployment. Below the frame is chain and a 226 kg (500 lb) anchor; two acoustic release packages can be seen on the sides of the system.

and held vertical by using subsurface flotation (Fig. 3). The pressure sensor in the AQUADOPP current meter measured 3 to 5 m depths and to the first order rose and fell with the tides due to the nearby surface floats. Each of the current meters produced a time-series of east- and north-going velocity vectors. Basic statistics (maximum, minimum, mean and standard deviation) were calculated for each data set for the three deployments (e.g. net conditions).

B. Load Cells

The second component of the field program included the deployment of nine load cells and recorders around net pen #4 and mooring components in the Southwest corner of the farm (Fig. 6) to measure forces in the anchor legs and the net pen attachment lines. Load cells with a 90-133 kN capacity were deployed on five of the anchor legs around the SW net pen. Load cells with a 44-66 kN capacity were attached to four lines mooring the net pen in the grid (Fig. 6).

Ten load cells were built as part of the University of New Hampshire Open Ocean Aquaculture demonstration project and successfully deployed from August 2000 through July 2002 on an offshore fish cage and mooring system [11] and [8]. The load cells were designed and constructed for underwater aquaculture operations by Sensing Systems Corporation of New Bedford, MA and were constructed with a working tension range of 0 to 133 kN, but survivable to 267 kN, to be compatible with the other components in the mooring. The load cells had an internal amplifier for the strain gauges so that a 0 to 2.5 volt signal sent through the Impulse underwater connector would be compatible with the Persistor recorder, and the higher voltage (rather than bridge voltages) would be less affected by connector resistance effects. The load cells were designed to be insensitive to torque that would be applied by standard ropes in the mooring system under varying tension. Six of these were refurbished for this study, and five deployed in the anchor lines (Fig 6.).

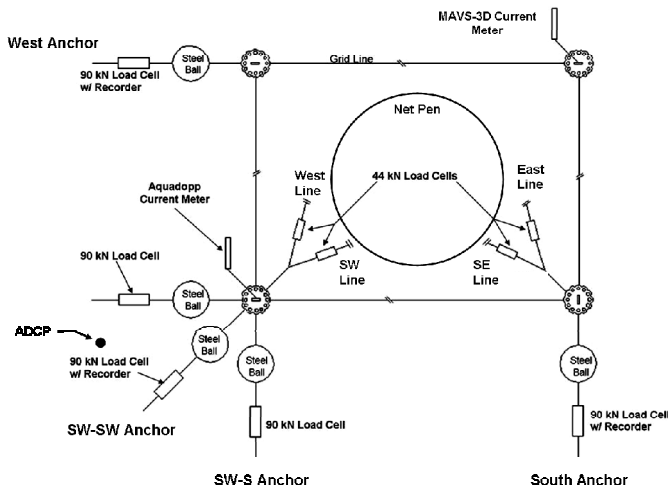


Figure 6: Instruments deployed at the Southwest grid corner. Five load cells and 3 recorders were installed on the anchor legs. Four load cells were attached to the net pen attachment lines, with recorders secured to the net pen stanchions. The current meter locations are also shown.

The anchor leg load cell and recorder systems were designed to be attached in-line with the mooring structure. Each load cell was attached to a steel strong back with an eye on each end (Fig. 7). The recorder and battery were contained in a PVC pressure case that is attached to the strong back, but could be recovered for data download and servicing by divers. For applications where several load cells would send signals to one recorder, a shorter strong back was used. The recorders were designed around the Persistor microcontroller that has an 8 channel 12-bit A/D and uses compact flash media for data storage. The system was powered by a 12-volt 80 ah battery capable of powering one load cell and recorder for approximately 1 year.

Four lower range load cells with a capacity between 44-66 kN were designed with similar strong backs, and compatible with the recorders. These load cells were deployed on the net pen attachment lines, with the recorders strapped to cage stanchions out of the water. These cases were designed to be water resistant and allow for intermittent shallow submersion, but not for sustained submersion at depth.

The recorder sampling rate was set to run on the hour for 20 minutes at 5 Hz, collecting 6,000 samples per “burst.” The burst-sampling scheme was selected in case if waves, as well as currents, were of importance. The ADCP also deployed at the site was configured to measure waves, but the results not reported because the wave elevations were negligible. The load cells were individually calibrated at Sensing Systems with a SensorTronics S/N 828531 Model 6001A20k-1177 standard. The load cell amplifiers were adjusted for a nominal 0.1-volt output under no load, and 2.5 volt output under full scale load (66 kN or 133 kN). The load cell “zero output” was verified during recorder preparation and the signal, current and voltage was recorded for documentation for each load cell before deployment.

After the field program, the load cells and recorders were calibrated at the Woods Hole Oceanographic Institution using a Baldwin Model 60-SC Universal Testing Machine with Admet digital readout and calibrated yearly by American Calibration and Testing. Least square regressions were fit to the calibration data, compared with the pre-deployment Sensing Systems calibrations and pre-and post-deployment zeros, and the most consistent results used to normalize the data.

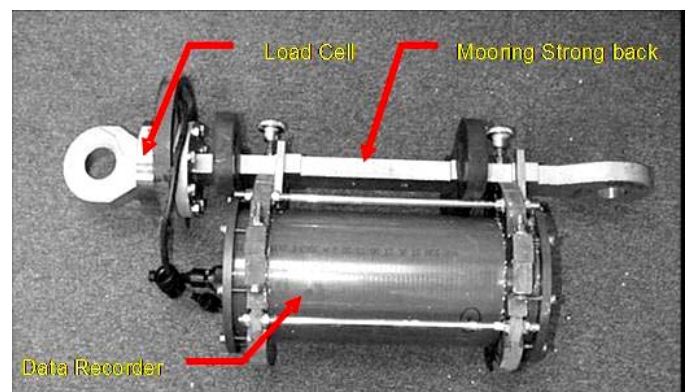


Figure 7: The load cell and strongback with diver serviceable recorder assembly as deployed at the site.

The five higher capacity load cells and 3 recorders were installed on the West (W), Southwest-West (SW-W), Southwest-Southwest (SW-SW), Southwest-South (SW-S) and the South (S) anchor legs (Fig. 6). The three corner load cells (SW-W, SW-SW, and SW-S) shared a recorder, connected by cables secured along the mooring system, whereas the adjacent anchor legs (W and S) had separate load cells and recorders. The strong backs and load cells were shackled into the mooring legs by picking the anchor chain up at one point, and then pulling the bottom of the legs together to give enough slack to shackle in the load cell system so that when the anchor chain was deployed, the load cell took the load and the spare chain was slack (Fig. 8). The recovery was the reverse of this process.

The four lower capacity load cells were placed on the net pen attachments identified as the West-, SW-, SE- and East Lines. The electrical cables used to connect the load cells to individual recorders were secured with the recorders to the net pen stanchions (Fig. 9). These load cells were attached to a second set of attachment lines so the original ones would not have to be removed (Fig. 10). The new attachment lines with the load cells were tensioned to take the load of the net pen, while the previously deployed lines were allowed to go slack.

III. PRELIMINARY RESULTS

A. Fish Farm Currents for Nets with Biological Fouling

The first deployment (condition #3) took place from 10/03/03 to 12/31/03 during the last three months of the salmon grow out cycle. The ADCP, AQUADOPP and MAVS current meters were deployed at the positions shown on Fig. 2 and 6. During this time period, an excessive amount of biological fouling was observed on the entire net pen and mooring system components. After recovery of the instruments, it became apparent that the AQUADOPP and MAVS current meters were also fouled. The raw data indicated that the MAVS current meter was more susceptible to fouling. The speeds from 10/3/03 to 10/31/03 are presented in Fig 11 since fouling affected the measurements after that time. Using this “clean”

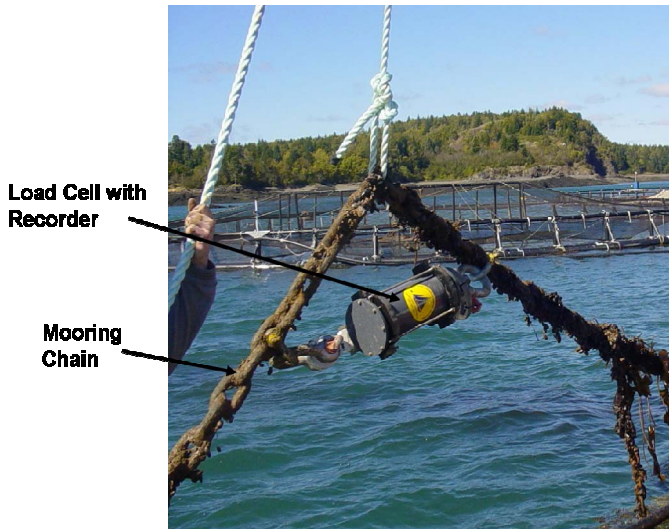


Figure 8: One of the higher capacity load cells with recorder installed on the south anchor leg.

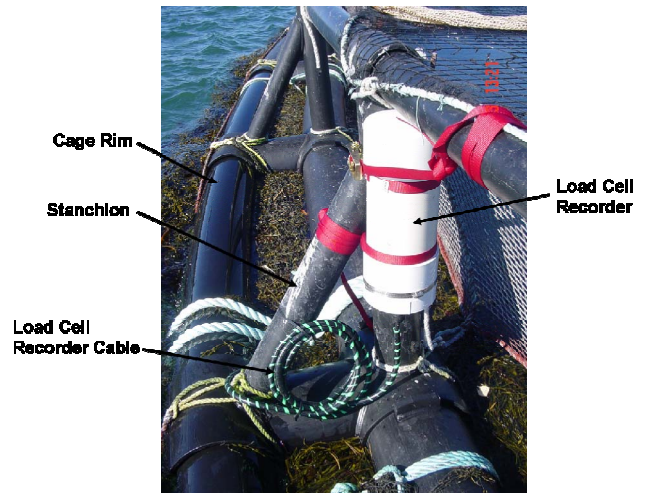


Figure 9: One of the lower capacity load cells and recorder attached to a net pen stanchion. The cable runs between the rings to the load cell attached to an attachment line (not shown).

section, the speeds was determined from the east and north components and the basic statistics (maximum, minimum, mean and standard deviation) calculated (Table 2).

Table 2: The basic statistics obtained from the clean speed time series measured with the ADCP, AQUADOPP and MAVS current meters.

Location	Max(m/s)	Min(m/s)	Mean(m/s)	Std(m/s)
ADCP	0.7636	0.0070	0.2233	0.1385
AQUADOPP	0.7682	0.0022	0.1859	0.1377
MAVS	0.4920	0.0014	0.1129	0.0868

Comparison of the speed statistics shows that a difference exists between the ADCP and AQUADOPP results with mean ADCP values approximately 17% higher. This indicates that the AQUADOPP, being closer to net pen #4, may be in slight



Figure 10: The net pen load cells were attached to an additional attachment line assembly. Bio-fouling on one of the existing line assemblies consisted of macro-algae with lengths nearly 10 m.

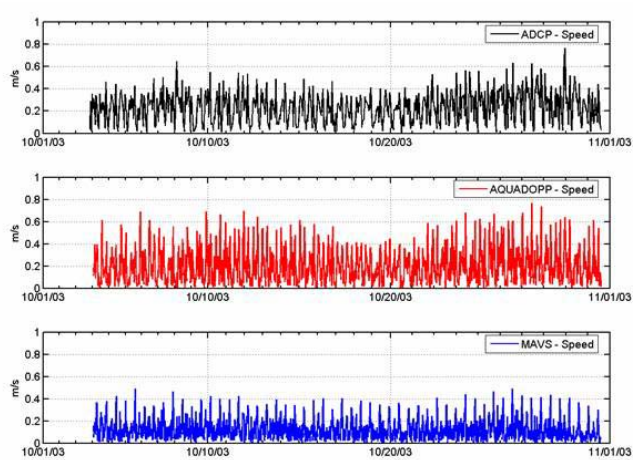


Figure 11: The current meter speed time-series from the ADCP, AQUADOPP and MAVS current meters deployed during the condition with fouled nets.

stagnation zone as flow deflects around the entire farm during the fouled condition. Evidence of flow deflection can also be seen by comparing the MAVS statistics with the other two current meters. The mean MAVS values were 50 and 40% less than the ADCP and AQUADOPP, respectively.

The currents are largely tidal as shown in the spectrum of the AQUADOPP east-going velocity record (Fig. 12). The largest energy is at the semidiurnal frequency, while the diurnal component is small. Nonlinear effects are indicated as higher harmonics of the twice a day tides (with 6 and 10 cycles per day highest, then 4, 8 and 12). This is not surprising for a shallow location near the Bay of Fundy with its large tides. The nonlinear effects result in a velocity record which is no longer sinusoidal (Fig. 13), but more pulse in nature. As the semidiurnal tide is the largest band, and the M2 the largest constituent, further analysis of this component is performed.

The one month data were analyzed [17] to obtain east and north components of the M2 constituent and represented in elliptical form as shown on Fig. 14. It is not as evident that

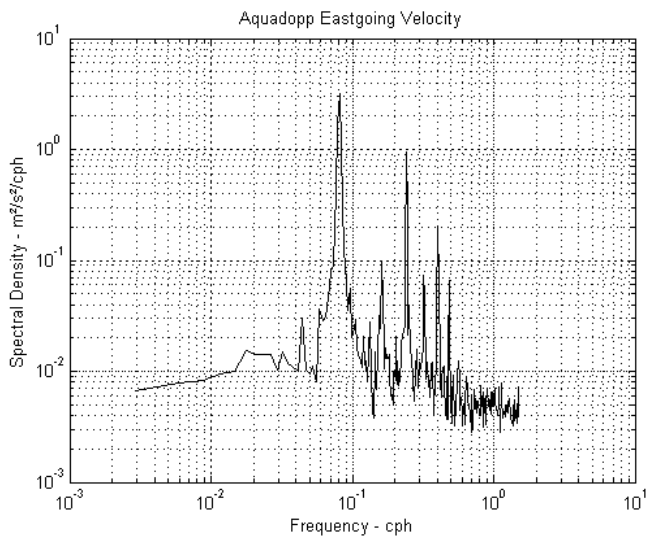


Figure 12: The power density spectrum for the east-going component of velocity from the AQUADOPP instrument is typical of the currents measured.

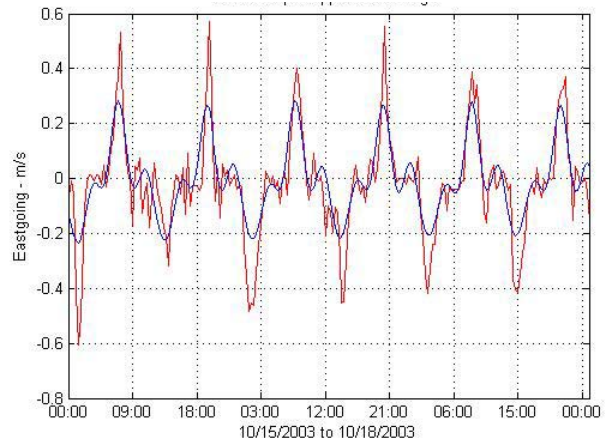


Figure 13. Detailed time series of the AQUADOPP east-going velocity component (red) and tidal prediction (blue) showing the nonlinearity of the tides.

current velocity reduction is occurring between the ADCP and AQUADOPP at the M2 frequency. Behind one net-pen the MAVS ellipse shows a substantial reduction and turning. However, as seen in Fig. 13, the tidal analysis under-predicts the current peaks. This implies that a tidal analysis is a poor predictor of the current peaks for modeling.

B. Fish Farm Currents with Smolt Nets Installed

The second deployment took place from 4/4/2004 to 6/7/2004. After the previous deployment, which ended 12/2003, all of the fish from the farm were harvested and the net pens and mooring gear removed from the site. During the winter months, all of the gear was serviced and cleaned. In April, it was all redeployed for the beginning of the grow-out cycle with smaller nets to contain the smolts. During this deployment period, the AQUADOPP, MAVS and S4 current meters were installed (Fig. 2). The MAVS data showed evidence of fouling and measurements appeared to be affected. From 5/4/2004 to 5/16/2004 the data acquired appeared to be “clean” and the speed time series shown in Fig. 15 and the statistics provided in Table 3.

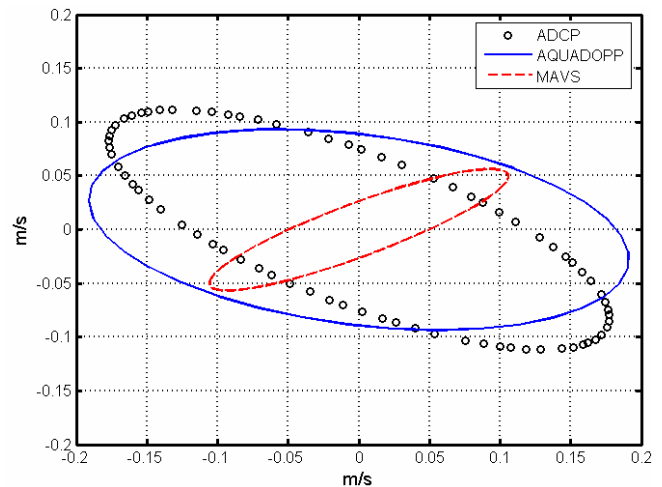


Figure 14: The M2 tidal ellipse comparison between the ADCP (circles), AQUADOPP (solid) and MAVS (dashed). The East and North components are represented by the x- and y-axes, respectively.

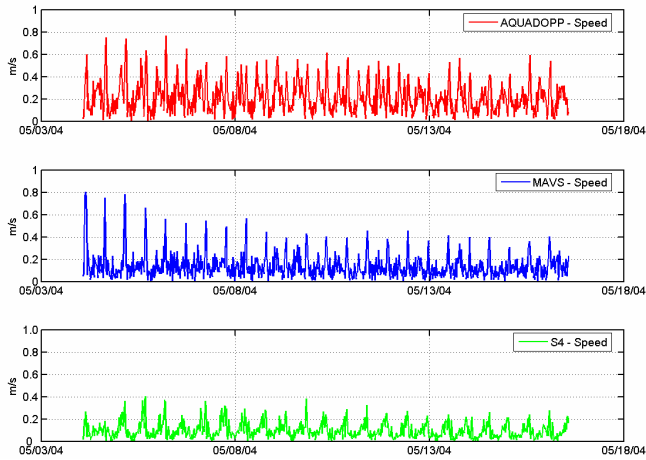


Figure 15: The speed time series results from the AQUADOPP, MAVS and S4 current meters deployed at the fish farm site during the condition with smolt nets.

Table 3: The basic statistics obtained from the clean speed time series measured with the AQUADOPP, MAVS and S4 current meters.

Location	Max(m/s)	Min(m/s)	Mean(m/s)	Std(m/s)
AQUADOPP	0.7671	0.0036	0.2103	0.1365
MAVS	0.8010	0.0030	0.1324	0.1062
S4	0.4021	0.0000	0.0967	0.0680

With the clean smolt and predator nets installed, flow reduction is clearly evident (Table 3). The percent difference between the AQUADOPP and MAVS mean value was 37%, which is less than the fouled condition. The S4 data shows a 54% reduction in mean from the AQUADOPP. The M2 tidal constituent amplitudes and the ellipses, (Fig 16.), also shows that current velocity reduction between the three locations.

C. Fish Farm Current with Standard Clean Nets

The third current meter deployment (condition #1) took place from 6/2004 to 9/2004. During this deployment, the smolt nets replaced by clean grow out and predator nets. The AQUADOPP, MAVS and S4 current meters were placed at the same locations, though the S4 current meter did not return

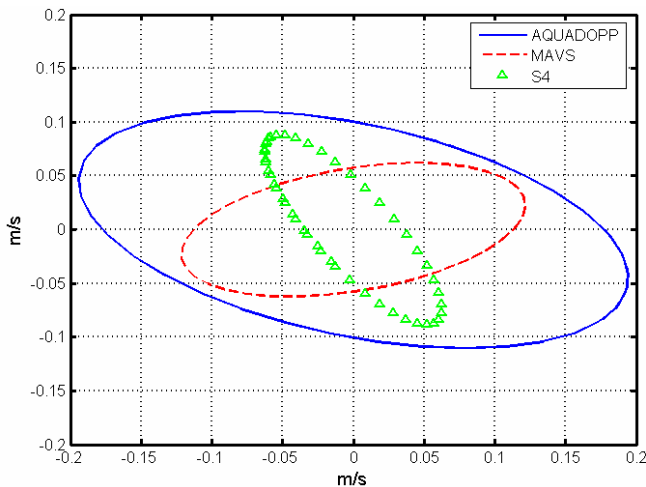


Figure 16: The M2 tidal ellipse comparison between the AQUADOPP (solid blue), MAVS (dashed red) and the S4 (green triangle). The East and North components are represented by the x- and y-axes, respectively.

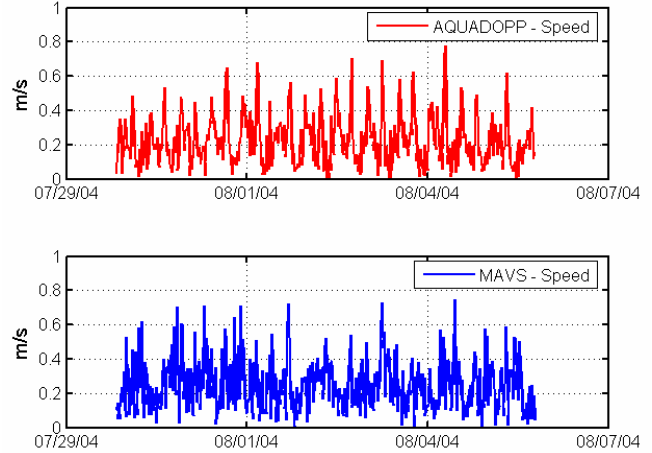


Figure 17: The speed time series results from the AQUADOPP and MAVS current meters deployed at the fish farm site during the condition with clean nets.

any information, and the MAVS instrument appeared to be excessively noisy (later traced to a damaged sensor head). A suitable duration was identified, however, where the data appeared to be clean (Fig. 17). Using the deployment time period between 7/29/2004 at 2000 and 9/5/2004 at 1840 UTC, the basic statistics are provided on Table 4.

Table 4: The basic statistics obtained from the clean speed time series measured with the AQUADOPP and MAVS current meters.

Location	Max(m/s)	Min(m/s)	Mean(m/s)	Std(m/s)
AQUADOPP	0.7762	0.0080	0.2177	0.1361
MAVS	0.7498	0.0061	0.2413	0.1484

The maximum velocity reduction from outside to inside is relatively small. (Note from Table 1 that the total net solidity for this case was 19.7%, approximately half of the smolt net condition.) The M2 tidal constituent ellipses (Fig. 18) do show a reduction between the two locations, but less than the fouled or smolt nets.

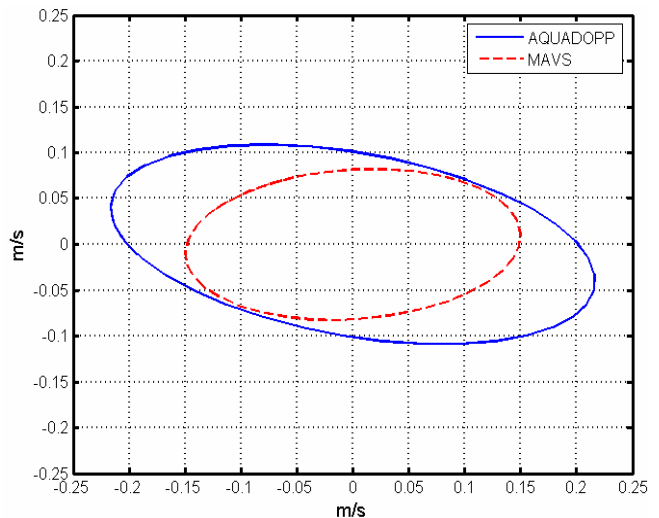


Figure 18: The M2 tidal ellipse comparison between the AQUADOPP (solid blue) and the MAVS current meters (dashed). The East and North components are represented by the x- and y-axes, respectively.

D. Mooring System and Cage Attachment Loads

In addition to the current meters, load cells were installed during the fouled, smolt and clean net conditions (Fig. 6). All nine load cells and seven data recorders were deployed at the farm site on 10/3/2003 (condition #3 – Fouled Nets). The instruments were recovered on 1/4/2004 and the data downloaded. Two of the load cells recorded reliable information. Clean data sets were obtained from the load cells located on the West and Southern anchor legs. Inspection of the stainless steel load cell housings showed strong evidence of severe crevice corrosion and therefore most of the instruments had salt water intrusion. The data acquired is listed in Table 5.

Table 5: The load cell data statistics obtained from the fouled, smolt and clean net deployments.

Position (Instrument)	Max (kN)	Mean (kN)
FOULED NETS		
West Anchor	56	7
South Anchor	51	9
SMOLT NETS		
West Line	10	2.6
SW Line	11	1.1
SE Line	13	3.5
East Line	6.4	-0.44
CLEAN NETS		
West Anchor	104	16
SW-W Anchor	37	6.3
SW-SW Anchor	36	9.7
SW-S Anchor	46	8.9
South Anchor	56	13
West Line	8.8	0.21
SW Line	9.9	0.94
SE Line	10.3	2.1
East Line	-	-

The end of the first deployment was also the end of the salmon 18-month growout cycle. Salmon farm best management practices suggest that the site should sit fallow for several months between classes of fish. This time was also used to refurbish/repair all of the load cells for the smolt net deployment. In April 2004, the mooring system and net pens of the farm were redeployed with smolt nets, four load cells were deployment with clean moorings and pens with smolt nets. The length of the second deployment period was from 4/28/2004 to 6/7/2004. The tensions are provided in Table 5.

In June 2004, the smolts had grown to a size where larger containment nets could be installed on each net pen. In this case, clean predator and containment nets were attached to the pens (condition #2 - Clean Nets). On 6/8/2004, nine load cells and seven data recorders were attached to the mooring (Fig. 6). The load cells operated from 6/8/2004 to 8/28/2004 and collected data until the compact flash cards filled. The 20 minute burst records were processed and statistic calculated and listed in Table 5.

The net pen attachment load cells showed similar results with maximum values up to approximately 13 kN. The tensions for the smolt net deployment were slightly higher. The fourth load cell (East Line) worked intermittently. The West anchor leg load cell recorded maximum values of 56 and 104 kN for the Fouled and Clean Net conditions, respectively. The

maximum load values recorded on the South anchor leg were between 51 and 56 kN. For the clean net condition, excessive high values may have been due to the operational staff over tensioning the West anchor leg. In the most southwest corner of the farm, an array of three anchor legs was deployed, each with an in-line load cell. All three of these load cells were connected through cables to one recorder. These load cells worked well recording maximum values ranging between 36 and 46 kN for the clean net condition. In general, there were no surprises or unusual findings in these data sets. The observations provide the data for checking with model results, and assessing the maximum tensions in the mooring lines due to drag on the whole fish farm system due to the currents.

IV. DISCUSSION

The current velocity measurements at each location were processed using basic statistics and for tidal harmonic constituents. For all three deployments, the maximum and mean velocities measured at the AQUADOPP location were approximately 0.76 m/s and 0.22 m/s, respectively. Examining the basic statistics for each of the deployment locations showed evidence of velocity reduction through the farm (though for the clean net condition, the values were nearly identical).

Tidal analysis also showed evidence of velocity reduction for each net condition. (Figs. 14, 16, and 18) This may have significant importance in the calculation of drag loads and therefore the specification of mooring components. Others [4], [7] have addressed these issues previously, but from the theoretical and physical modeling perspective. While [18] looked at the drag characteristic of 1-m square net panels with varying levels of biological fouling. In this case, actual measurements were made in an operating fish farm during conditions with different net solidity characteristics.

As expected, the M2 constituent was found to be the dominant tidal component. Most circulation studies involving hydrodynamic models built for the region are forced using M2 tidal characteristics [19], [16], and [20]. Results from the measurements taken as part of this study, however, showed evidence of strong shallow water or tidal harmonic influence. According to [21] and [22], among others, the contribution of the higher harmonic components is important in the accurate representation of velocities in estuaries that are relatively shallow with large tidal amplitudes. This data also showed that future hydrodynamic modeling studies of the area should consider the nonlinear, higher harmonic influence, especially since many of these models are used to calculate the transport of fish farm wastes and diseases.

Under normal tidal current conditions, the maximum anchor loads “experienced” by the system were approximately 104 kN. These loads occurred on the West side of the system, which was consistent with discussions with operational personnel that have had to reset gear at this location on multiple occasions. The components used on the western anchor legs consist of 1-1/2” long link steel chain with an approximate working load (new) of 150 kN. So the primary mooring components were specified appropriately.

The attachment lines, which consist of 1 inch (24 mm) copolymer (polypropylene and polyethylene fiber) in a three-strand construction, have a manufacturer's average tensile strength of 97 kN. Maximum load values measured were approximately 13 kN so the components were also sufficient.

V. CONCLUSION

The results of this study clearly show evidence of flow reduction through the farm for the fouled, smolt and clean net conditions. The reduction also appears to be a function of net solidity. In a 20 net pen system, the reduced velocities could have an effect on the drag load calculation. This will become increasingly more important when applying finite element models that use a form of Morison equation for load calculation. If an accurate representation of the velocity field and net solidity is known, specification of components can be optimized.

For the near shore fish farm site, the measured operating loads were well within the capabilities of the components. If the same farm was to be deployed in an exposed or open ocean location, the same components or farm configuration may not be suitable. The load data set acquired as part of this study can serve as a baseline for validating large fish farm numerical models, which in turn can then be applied for more extreme environmental conditions.

Another significant result was obtained from the tidal harmonic analysis. Each of the eight current meter data sets showed that strong harmonic or overtide influence exists in the region. The region contains a total of 26 finfish lease sites. Hydrodynamic models used for the transport of aquaculture wastes should consider these tidal components as part of the forcing boundary conditions.

The current velocity data sets may also be used with computational fluid dynamic methods to examine flow field details through and around the farm with the same net solidity characteristics and conditions. Flow characteristics have an influence on the oxygen exchange within the farm, which influences fish growth rates.

ACKNOWLEDGEMENTS

The authors would like to acknowledge the operational and management staff at the Heritage Salmon site in Broad Cove located in Eastport, ME USA. The authors would also like to acknowledge Professors B. Celikkol, M.R. Swift, K.C. Baldwin and I. Tsukrov for advice and support. Additional thanks go to G. McGillicuddy, G. Rice and C. Turmelle for technical assistance.

REFERENCES

[1] Le Bris, F and D. Marichal. (1998) Numerical and experimental study of submerged supple nets: Applications to fish farms. J. Mar. Science and Tech. Vol 3, pp. 161-170.
 [2] Tsukrov, I., Eroshkin, O., Fredriksson, D. W., Swift, M.R. and Celikkol, B., (2003). Finite element modeling of net panels using consistent net element. Ocean Eng. 30: pp. 251 – 270.

[3] Lader, P.F. and A.L. Fredheim. (2003) *Modeling of Net Structures in 3D waves and currents*. In C.J. Bridger and B.A. Costa-Pierce, editors. Open Ocean Aquaculture: From Research to Commercial Reality. The World Aquaculture Society, Baton Rouge, Louisiana, United States. pp 177-189.
 [4] Aarnses, J., H. Rudi and G. Loland (1990). *Current Forces on Cage, Net Deflection*. In: Engineering for Offshore Fish Farming. Thomas Telford. pp 137-152.
 [5] Fredriksson, D.W., J. DeCew, M.R. Swift, I. Tsukrov, M.D. Chambers, and B. Celikkol. (2004). The Design and Analysis of a Four-Cage, Grid Mooring for Open Ocean Aquaculture. Aqua. Eng. Vol 32/1 pp 77-94.
 [6] Lader, P.F. and B. Enerhaug. (2005). *Experimental Investigation of Forces and Geometry of a Net Cage in Uniform Flow*. Special Issue On Open Ocean Aquaculture Engineering. IEEE J. Oceanic. Eng. Vol. 30, No. 1 pp 79-84.
 [7] Loland, G. (1991). *Current Forces on and Flow Through Fish Farms*. Ph.D. Thesis, Division of Marine Hydrodynamics at the Norwegian Institute of Technology. p. 149.
 [8] Fredriksson, D.W., M.R. Swift, J.D. Irish, I. Tsukrov and B. Celikkol. (2003a) *Fish Cage and Mooring System Dynamics Using Physical and Numerical Models with Field Measurements*. Aqua. Eng. Vol 27, No. 2, pp. 117-146.
 [9] DeCew, J., D.W. Fredriksson, L. Bougrov, M.R. Swift, O. Eroshkin and B. Celikkol. (2005). Numerical and Physical Modeling of a Modified Gravity Type Cage and Mooring System. IEEE J. of Ocean. Eng. Vol. 30, No. 1 pp 47-58.
 [10] Colbourne, D.B and Allen, J.H., 2001. Observations on motions and loads in aquaculture cages from full scale and model scale measurements. Aquacult. Eng. 24 (2), 129 – 148.
 [11] Irish, J.D., M. Carroll, R. Singer, A. Newhall, W. Paul, C. Johnson, N. Witzell, G. Rice and D.W. Fredriksson. (2001). *Instrumentation of Open Ocean Aquaculture Monitoring*. Woods Hole Oceanographic Institution, Technical Report WHOI-2001-15. p. 95.
 [12] Fredriksson, D.W., M.R. Swift, J.D. Irish and B. Celikkol. (2003b). *The Heave Response of a Central Spar Fish Cage* Transactions of the ASME, J. of Off. Mech. and Arct. Eng. Vol 25, pp 242- 248.
 [13] Fredriksson, D.W., M.J. Palczynski, M.R. Swift, J.D. Irish and B. Celikkol. (2003c). *Fluid Dynamic Drag of a Central Spar Cage* in C.J. Bridger and B.A. Costa-Pierce, editors. Open Ocean Aquaculture: From Research to Commercial Reality. The World Aquaculture Society, Baton Rouge, Louisiana, United States. pp 151-168.
 [14] Fredriksson, D.W. , M.R. Swift, O. Eroshkin, I. Tsukrov, J.D. Irish, and B. Celikkol. (2005). *Moored Fish Cage Dynamics in Waves and Currents*. Special Issue On Open Ocean Aquaculture Engineering. IEEE J. Oceanic. Eng. Vol. 30, No. 1 pp 28-36.
 [15] Garrett, C. (1974). Normal modes of the Bay of Fundy and Gulf of Maine, Can. J. Earth Sci., 11, 549-556.
 [16] Dudley, R.W., V.G Panchang and C.R. Newell. (2000) Application of a Comprehensive Modeling Strategy for the Management of Net-pen Aquaculture Waste Transport. Aquaculture, (187) 3-4, pp. 319-340.
 [17] Pawlowicz, R, Beardsley, B and S. Lentz, (2002) "Classical tidal harmonic analysis including error estimates in MATLAB using T_TIDE", Computers and Geosciences 28 (2002), 929-937.
 [18] Swift, M.R., Fredriksson, D.W., Unrein, A., Fullerton, B., Patursson, O., Baldwin, K., (2006). Drag Force Acting on Biofouled Net Panels. Aqua. Eng. (accepted).
 [19] Panchang, V.J., Cheng, G. and C. Newell. (1997). Modeling Hydrodynamics and Aquaculture Waste Transport in Coastal Maine. Estuaries. Vol 20, No. 1, pp 14-41.
 [20] Brooks, D.A., M.W. Baca Y.T. Lo. (1999) Tidal Circulation and Residence Time in a Macrotidal Estuary: Cobstock Bay, Maine. Est., Coast. and Shelf Science, 49, 647-665.
 [21] Aubrey, D.G., Speer, P.E. (1985). A study of non-linear tidal propagation in shallow inlet/estuarine systems, Part I: observations. Estuarine, Coastal and Shelf Science 21, 185-205.
 [22] Blanton, J.O., Lin, G., and S.A. Eston (2002). Tidal current asymmetry in shallow estuaries and tidal creeks. Cont. Shelf Research 22, 1731-1743.